Journal Name

ARTICLE

Well-defined SiO_2-coated Fe_2Co nanoparticles prepared by reduction with CaH_2

Received 00th January 20xx,
Accepted 00th January 20xx

DOI: 10.1039/x0xx00000x

www.rsc.org/

S. Yamamoto*[a] and M.Tsujimoto[a]

Well-defined SiO_2-coated Fe_2Co nanoparticles have been successfully prepared by reducing SiO_2-coated $CoFe_2O_4$ nanoparticles with CaH_2. Lowering of the reducing temperature by the use of CaH_2 is essential to keep the well-defined morphology of the starting nanoparticles intact. Surface modification with a silane-coupling agent having COOH groups has led to excellent aqueous dispersibility that facilitates subsequent functionalization with a variety of molecules via well-established processes such as EDC/NHS chemistry. Thus-obtained SiO_2-coated Fe_2Co nanoparticles equipped with controlled morphology, corrosion resistivity, soft magnetic properties, and easy post-functionalization are expected to serve as a building block for electromagnetic, biological, and medical applications.

Introduction

Iron-cobalt alloys ($Fe_{1-x}Co_x$, $x < 0.75$) with the body-centered cubic (bcc) structure are an important class of soft magnetic materials known to have the highest saturation magnetization (M_s ~ 240 emu/g) at x = 0.35. Nanoparticles with such a high-M_s and low-anisotropy are especially important for electromagnetic applications.[1,2] They also may have applications in the fields of bio- and medical-sciences and technologies, *e.g.*, magnetic purification of biologically important staffs, magnetically guided drug delivery, hyperthermia and magnetic resonance imaging (MRI, T_2-imaging) since the performance in such applications is known to be strongly dependent on M_s.[3]

Stabilization of these nanoparticles against oxidation is practically important since they lose their superior magnetic properties once oxidized. Composite materials composed of $Fe_{1-x}Co_x$ nanoparticles embedded in protecting oxides such as SiO_2 and Al_2O_3 have been prepared by sol-gel procedures,[4-8] in which precursory sols containing Fe- and Co-cations are heat-treated under reducing atmospheres at high temperatures (typically 800 °C). Such a method gives several advantages, *e.g.*, high stability against oxidation, formability and compositional and structural homogeneity. However, poor control over the size and morphology of the magnetic particles caused by thermal coagulation and fusion has been problematic since magnetic properties are strongly affected by these factors. Therefore, this method has found few applications in bio- and medical-sciences and technologies where free nanoparticles dispersible in aqueous solutions are needed. Recently, we have succeeded in preparing SiO_2-coated α-Fe nanoparticles with well-defined morphologies by using CaH_2 as a reductant.[9,10] This hydride has recently attracted much attention in the field of solid state chemistry as an easy-to-handle solid reductant working efficiently at low temperatures.[11-17] In the present case the greatest benefit brought by this reductant is drastic lowering of the reducing temperature, which makes it possible for the nanoparticles to be free from aggregation and coalescence and keep their original morphology intact. Here, we report the preparation of SiO_2-coated Fe_2Co nanoparticles via reduction of SiO_2-coated $CoFe_2O_4$ nanoparticles by using CaH_2 (Scheme 1). We also tried to modify their surface with a COOH-carrying silane coupling agent (COOH-silane). The presence of this surface group greatly facilitates subsequent modifications with a variety of functional molecules, which are very important in bio- and medical-sciences and technologies.

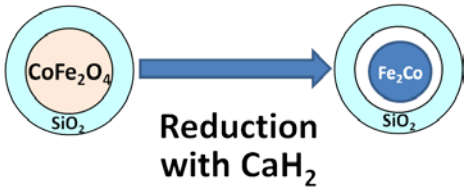

Scheme 1. Schematic representation of preparation of SiO_2-coated Fe_2Co nanoparticles by reducing SiO_2-coated $CoFe_2O_4$ nanoparticles with CaH_2.

Experimental

Preparation of $CoFe_2O_4$ nanoparticles

The $CoFe_2O_4$ nanoparticles were prepared using an adaptation of the reported procedure.[18] Briefly, 4 mmol of $Fe(acac)_3$, 2 mmol of $Co(acac)_2$, 30 mmol of 1,2-hexadecanediol, 18 mmol of oleic acid, 18 mmol of oleylamine, and 60 mL of benzyl

[a] Institute for Integrated Cell-Material Sciences, Kyoto University, Yoshida Ushinomiya-cho, Sakyo-ku, Kyoto, Kyoto 606-8501, Japan

Electronic Supplementary Information (ESI) available: [complementary data(Figure S1 and S2)]. See DOI: 10.1039/x0xx00000x

ether were combined and stirred under N_2 atmosphere. The mixture was heated to 200 ^{o}C for 2 hrs and then, under a blanket of N_2, heated to reflux for 1 h. The black mixture was cooled to room temperature by removing the heat source. Under ambient conditions, 40 mL of ethanol was added to the mixture, when a black material was precipitated. The precipitate was separated by centrifugation and then dispersed in hexane containing an appropriate amount of oleic acid. The mixture was centrifuged and the supernatant was decanted off. The desired product was precipitated by adding ethanol to the residual and separated from the solvent by centrifugation and decantation, which was then dried in vacuum overnight. The nanoparticle has Iron/cobalt ratio of 2/1, as determined by inductively coupled plasma-mass spectrometry (ICPS-8100, Shimadzu).

SiO_2-coating of $CoFe_2O_4$ nanoparticles

Coating of SiO_2 on the $CoFe_2O_4$ nanoparticles was performed based on the procedures described elsewhere.[9,10] In brief, to the cyclohexane solution (1170 g) containing polyoxyethylene(5)nonylphenyl ether (56.7 g) and the $CoFe_2O_4$ nanoparticles (30 mg), ammonium hydroxide (28%, 11.1 ml) was added and magnetically stirred for 30 min to form a transparent, brown reverse microemulsion. Then, tetraethyl orthosilicate (6.3 g) was added, and the reaction was continued for 24 hrs at room temperature. The resulting SiO_2-coated $CoFe_2O_4$ nanoparticles were precipitated by adding ethanol to the reaction solution. They were collected by a magnet, washed with ethanol, and dried in vacuum.

Reduction with CaH_2

The reduction was done according to the method described elsewhere.[9,10] In brief, the SiO_2-coated $CoFe_2O_4$ nanoparticles and a four-weight excess of CaH_2 were finely ground in a N_2-filled glove box, sealed in an evacuated Pyrex tube, and heated for 12 hrs at 500 ^{o}C unless otherwise noted. Residual CaH_2 and CaO produced during the reduction were washed out with an NH_4Cl/methanol solution under air.

Modification with COOH-silane

To a 40 wt% ethanolic aqueous solution (30 g) of the SiO_2-coated Fe_2Co nanoparticles (20 mg), COOH-silane (0.3 g, N-(trimethoxysilylpropyl) ethylenediamine triacetic acid trisodium salt) (35% in water, Gelest) was added and the resulting mixture was kept at 80 ^{o}C for 3 days while stirring. The resulting nanoparticles were collected by centrifugation and washed with water, and collected again by centrifugation. The collected powder was redispersed in water and stored at room temperature.

Estimation of content of magnetic elements (Fe and Co) in the SiO_2-coated nanoparticles

The amount of magnetic elements in the sample was determined by thermogravimetry (TG, TG-DTA2000SA, Bruker AXS). The SiO_2-coated $CoFe_2O_4$ nanoparticles were transformed to SiO_2-coated $CoFe_2O_{4.5}$ nanoparticles by oxidization at 500 ^{o}C for 10 hrs in a stream of O_2, which were subsequently reduced in a stream of H_2 at 700 ^{o}C to SiO_2-coated Fe_2Co. The amount of magnetic elements in the initial sample was calculated from the decrease in weight on the reduction by assuming that SiO_2 remained intact during the reduction.

Other characterization methods

Low and high magnification transmission electron microscopic (TEM) observations were performed by using a JEOL JEM-1010D and a JEOL JEM-2200FS, respectively. TEM specimens were prepared by dropping a particle-containing solution on a carbon-coated copper grid. Powder X-ray diffraction (XRD) measurements were performed using a Bruker New D8 ADVANCE with Cu K_α radiation (λ = 0.154 nm). Magnetic properties were characterized by using a SQUID magnetometer (MPMS-XL, Quantum Design). Infrared (IR) spectra were collected on JASCO FT/IR-4200. The samples were each mixed with KBr and compressed into pellets.

Results and discussion

Figure 1 shows XRD patterns taken before and after the reduction. It is clear that $CoFe_2O_4$ was replaced by Fe_2Co with bcc structure. The broad peak around 2θ = 22 ^{o} is from the amorphous SiO_2 shell. We tried reduction at lower temperatures. As shown in Figure S1(a) in Electric Supplementary Information (ESI), Fe_2Co core formed even at 250 ^{o}C in 12 hrs. The average crystallite size (CS) of the Fe_2Co core estimated by using the Scherrer formula was *ca.* 4.4 ~ 5.5 nm. Higher reaction temperature seems to give larger CS probably due to better crystallinity (Figure S1b in ESI).

Here we briefly discuss about the possible reduction mechanism. The mechanism of reduction reactions of transition metal oxides using alkali and alkali earth hydrides was recently studied in detail by Kobayashi *et al*.[19] It was explained that the reduction proceeds by *in-situ* generated H_2

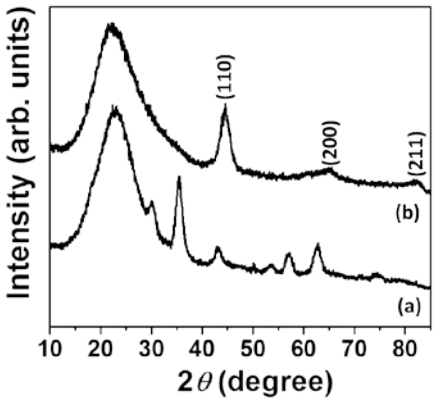

Figure. 1. XRD patterns of the sample (a) before and (b) after the reduction.

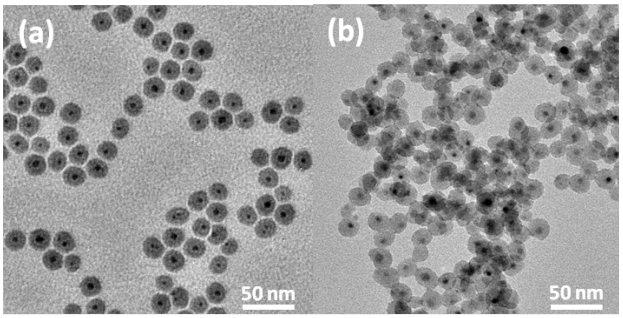

Figure. 2. Low magnification TEM images of the sample (a) before and (b) after the reduction.

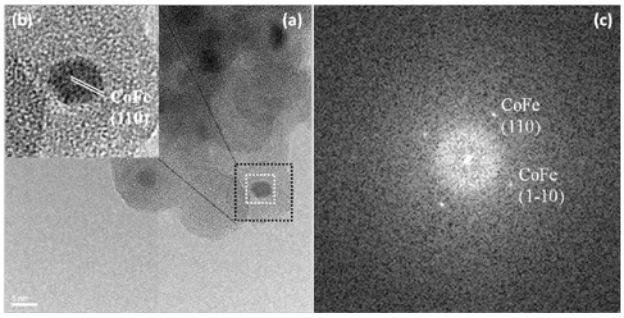

Figure. 3. (a) High magnification TEM image of the SiO_2-coated Fe_2Co nanoparticles, (b) enlarged image of the area surrounded by black dotted line in (a), and (c) an FFT image of the area surrounded by white dotted line in (a)

and, to a lesser extent, getter mechanism, since the reduction reaction proceeds in some cases even when the pristine oxides are physically separated from the reductant.[9,10,19] Similarly, in our system, $CoFe_2O_4$ nanoparticle is separated from the surrounding CaH_2 by the gas-permeable shell layer of SiO_2. We consider the reaction mechanism in our system is similar.

The low magnification TEM images taken before and after the reduction (Figures 2(a) and (b)) clearly show that the particles keep their original overall shapes and sizes. The diameters of the core particles before and after the reduction were estimated to be 6.1 ± 1.2 and 4.8 ± 0.7 nm, respectively, as averaged over 100 particles. The core particles shrink during the reduction due to removal of the oxygen atoms, yielding a clearance gap between the core and the SiO_2 shell as schematically shown in Scheme 1. The estimated diameter of the Fe_2Co cores is in good agreement with the expected volume shrinkage upon reduction ($V(1/3Fe_2Co)/V(1/3CoFe_2O_4)$ ~ 0.5). The clearance gap cannot be clearly seen in the present case possibly because of poor contrast arising from its small size, although it was clearly seen for larger particles treated in the previous works.[9,10]

Figures 3(a) and (b) show high magnification TEM images of the SiO_2-coated Fe_2Co nanoparticles after exposure to air (*ca.* 10 days). As shown in Figure 3(b), (110)-lattice fringes can be seen throughout the core particle revealing single crystalline nature of the Fe_2Co core (see also Figure S2 in ESI

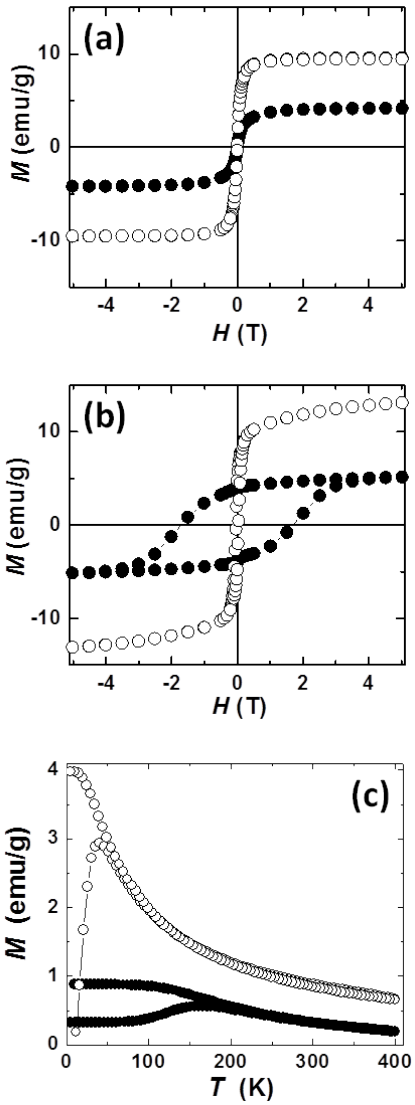

Figure. 4. Magnetic properties of the sample before (solid symbols) and after (open symbols) the reduction. Hysteresis loops measured at (a) 300 and (b) 5 K. (c) ZFC-FC curves measured under an external magnetic field of 100 Oe.

for the enlarged image). Figure 3(c) shows a fast Fourier transform (FFT) image of the core particle. Any crystalline oxide phase was not detected, but reoxidation during exposure to air was evidenced by a decrease in M_s as described later. This is because the SiO_2 shell includes open micropores. We observed such reoxidation also for SiO_2-coated α-Fe nanoparticles where the formation of crystalline oxide phase, FeO, was observed.[10] Absence of crystalline oxide phases in the FFT image may be due to formation of very thin oxide layer with low crystallinity.

Magnetic hysteresis (*M*-*H*) loops of the sample before and after the reduction measured at 5 and 300 K are shown in Figures 4(a) and (b), respectively. Here, *M* and *H* denotes magnetization per unit mass of the whole sample and external magnetic field, respectively. These figures clearly show that

Table 1. Changes in magnetic properties upon reduction.

sample	M_s[a] [emu/g]		$H_{c,5K}$[b] [T]	T_B[c] [K]
	300 K	5 K		
Before reduction	5.6	6.9	1.70	165
After reduction	12.8	17.5	0.04	49

a) Saturation magnetization defined as the magnetization at 5 T.

b) Coercivity at 5 K.

c) Blocking temperature defined as the temperature where ZFC curve shows the maximum.

both field-dependent magnetic properties are drastically changed upon reduction (see also Table 1) because of the transformation of the hard magnet with a small M_s, $CoFe_2O_4$, to the soft magnet with a large M_s, Fe_2Co.

The stability against oxidation in air at room temperature was studied for six samples reduced at different temperatures through intermittent magnetization measurements over 30 days (see Figure S3 in ESI). The decrease in M_s due to reoxidation ranged from *ca.* 20 % (reduced at 500 °C) to *ca.* 40 % for the others after 30 days. It seems the samples prepared at higher reaction temperatures have slighter reoxidaiton probably due to the better crystallinity. The decrease is not monotonous and almost ceases in ~ 25 days. A metal-core/oxide-shell structure seems to be stabilized. Estimation of the oxidized layer thickness from the magnetization data is rather difficult: saturation magnetization per magnetic elements (Fe and Co) at 300 K was estimated to be 64 emu/g based on the TG analysis, which revealed amount of the magnetic elements in the sample to be 15 wt%. This is even lower than the bulk saturation magnetization of $CoFe_2O_4$ at the same temperature (80.8 emu/g).[20] The oxidized layer seems to have very low saturation magnetization due to the low crystallinity, as indicated by the high magnification TEM study (see Figure 3(c)).

Figure 4(c) shows the temperature dependence of magnetization measured on heating after zero field-cooling (ZFC) and on field-cooling (FC). The field applied was 100 Oe. It is clear that field-dependent magnetic properties are also drastically changed upon reduction. If it is assumed that the ZFC and FC curves deviate from each other at the blocking temperature (T_B), T_B decreases from 165 to 49 K, indicating transformation of the hard magnetic $CoFe_2O_4$ to soft magnetic Fe_2Co.

Blocking temperature is related to magnetic anisotropy through the following relation:

$$T_B = KV/25k_B \quad (1)$$

Here, K, V, and k_B denote effective magnetic anisotropy constant, volume of the nanoparticle, and Boltzmann constant

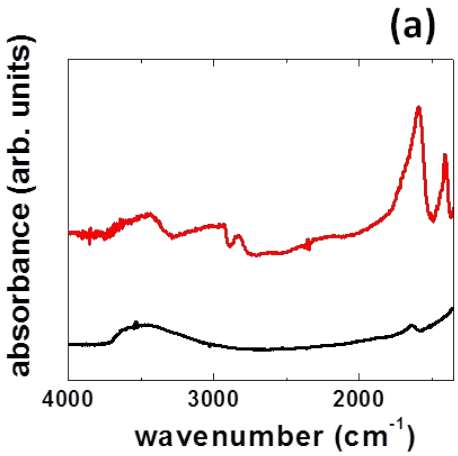

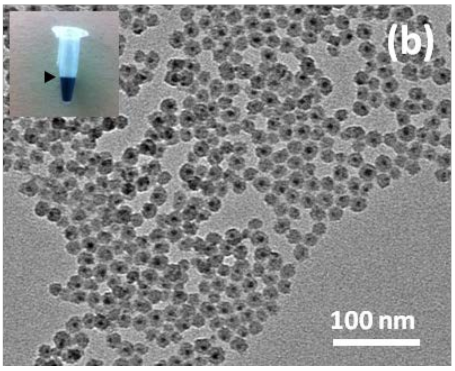

Figure. 5. (a) IR spectra of the SiO_2-coated Fe_2Co nanoparticles before (black line) and after (red line) the modification with COOH-silane, (b) low magnification TEM image of the nanoparticles after the modification with COOH-silcane. Inset shows a photo of a bottle of aqueous dispersion. The triangle indicates the fluid level.

(1.38 X 10^{-23} [J/K]), respectively. By using eq.(1) and an average particle volume estimated assuming that the particles have spherical shape and the diameter equal to that determined by TEM analyses (4.8 nm), K of the SiO_2-coated Fe_2Co nanoparticles was determined to be 3 X 10^5 [J/m^3]. This value is much higher than that of the Fe_2Co in the bulk form (*ca.* 3 X 10^4 [J/m^3][21]). Such changes in K were often observed for magnetic nanoparticles since surface contribution to anisotropy is much higher than in the bulk.[4,22]

We then tried to modify the surface of thus-obtained SiO_2-coated Fe_2Co nanoparticles with COOH-silane. Figure 5(a) shows IR spectra of the sample before and after the modification. After the modification intense absorption peaks assigned to the C=O and C-H stretching modes appear at around 1600 and 2900 cm^{-1}, respectively, showing successful introduction of COOH-silane. Upon introduction of COOH groups, surface properties drastically changed. Most importantly, the nanoparticles have gained aqueous dispersibility (see Figure 5b).

Conclusions

We have successfully prepared well-defined SiO_2-coated Fe_2Co nanoparticles by CaH_2-mediated reduction of SiO_2-coated $CoFe_2O_4$ nanoparticles. The use of CaH_2 is essential to keep well-defined morphologies of the pristine nanoparticles intact as the H_2 gas-treated sample heavily sintered to lose their pristine shape (Figure S4 in ESI). The introduction of COOH-group has been found to lead to excellent aqueous dispersibility, which also enables subsequent functionalization with a variety of molecules via well established processes such as EDC/NHS chemistry. The SiO_2-coated Fe_2Co nanoparticles equipped with controlled morphology, corrosion resistivity, soft magnetic properties and easy post-functionalization are expected to serve as a building block for electromagnetic, biological, and medical applications.

Acknowledgements

The present work was partly supported by KAKENHI (No. 24681022).

Notes and references

1 S. Ohnuma, H. J. Lee, N. Kobayashi, H. Fujimori and T. Matsumoto, *IEEE Trans. Magn.*, 2001, **37**, 2251.
2 S. Russek, P. Kabois, T. Silva, F. B. Mancoff, S. D. Wang, Z. Qian and J. M. Daughton, *IEEE Trans. Magn.*, 2001, **37**, 2248.
3 Q. A. Pankhurst, J. Connolly, S. K. Jones and J. Dobson, *J. Phys. D: Appl. Phys.*, 2003, **36**, R167.
4 A. Casu, M. F. Casula, A. Corrias, A. Falqui, D. Loche, S. Marras and C. Sangregorio, *Phys. Chem. Chem. Phys.*, 2008, **10**, 1043.
5 G. Ennas, M. F. Casula, A. Falqui, D. Gatteschi, G. Marongiu, G. Piccaluga, C. Sangregorio and G. Pinna, *J. Non-Cryst. Solids*, 2001, **293-295**, 1.
6 M. F. Casula, A. Corrias and G. Paschina, *J. Mater. Chem.*, 2002, **12**, 1505.
7 M. F. Casula, A. Corrias, A. Falqui, V. Serin, D. Gatteschi, C. Sangregorio, C. De Julian Fernandez and G. Battaglin, *Chem. Mater.*, 2003, **15**, 2201.
8 G. Ennas, A. Falqui, S. Marras, C. Sangregorio and G. Marongiu, *Chem. Mater.*, 2004, **16**, 5659.
9 S. Yamamoto, G. Ruwan, Y. Tamada, K. Kohara, Y. Kusano, T. Sasano, K. Ohno, Y. Tsujii, H. Kageyama, T. Ono and M. Takano, *Chem. Mater.*, 2011, **23**, 1564.
10 K. Kohara, S. Yamamoto, L. Seinberg, T. Murakami, M. Tsujitmoto, T. Ogawa, H. Kurata, H. Kageyama and M. Takano, *Chem. Commun.*, 2013, **49**, 2563.
11 M. A. Hayward, E. J. Cussen, J. B. Claridge, M. Bieringer, M. J. Rosseinsky, C. J. Kiely, S. J. Blundell, I. M. Marshall and F. L. Pratt, *Science*, 2002, **295**, 1882.
12 Y. Tsujimoto, C. Tassel, N. Hayashi, T. Watanabe, H. Kageyama, K. Yoshimura, M. Takano, M. Ceretti, C. Ritter and W. Paulus, *Nature*, 2007, **450**, 1062.
13 C. Tassel, T. Watanabe, Y. Tsujimoto, N. Hayashi, A. Kitada, Y. Sumida, T. Yamamoto, H. Kageyama, M. Takano and K. Yoshimura, *J. Am. Chem. Soc.*, 2008, **130**, 3764.
14 H. Kageyama, T. Watanabe, Y. Tsujimoto, A. Kitada, Y. Sumida, K. Kanamori, K. Yoshimura, N. Hayashi, S. Muranaka, M. Takano, M. Ceretti, W. Paulus, C. Ritter and G. André, *Angew. Chem., Int. Ed.*, 2008, **47**, 5740.
15 T. Yamamoto, Z. Li, C. Tassel, N. Hayashi, M. Takano, M. Isobe, Y. Ueda, K. Ohoyama, K. Yoshimura, Y. Kobayashi and H. Kageyama, *Inorg. Chem.*, 2011, **50**, 3988.
16 L. Seinberg, S. Yamamoto, R. Gallage, M. Tsujimoto, Y. Kobayashi, S. Isoda, M. Takano and H. Kageyama, *Chem. Commun.*, 2012, **48**, 8237.
17 L. Seinberg, S. Yamamoto, M. Tsujimoto, Y. Kobayashi, M. Takano and H. Kageyama, *Chem. Commun.*, 2014, **50**, 6866.
18 S. Sun, H. Zeng, D. V. Robinson, S. Raoux, P. M. Rice, S. X. Wang and G. Li, *J. Am Chem. Soc.*, 2004, **126**, 273.
19 Y. Kobayashi, Z. Li, K. Hirai, C. Tassel, F, Loyer, N. Ichikawa, N. Abe, T. Yamamto, Y. Shimakawa, K. Yoshimura, M. Takano, O. J. Hernandez and H. Kageyama *J. Solid State Chem.*, 2013, **207**, 190.
20 K. Maaz, A. Mumtaz, S. K. Hasanain, A, Ceylan, *J. Magn. Magn. Mater.*, 2007, **308**, 289.
21 Ch. Kuhrt and L. Schultz, *J. Appl. Phys.*, 1992, **71**, 1986.
22 T. Ninjbadgar, S. Yamamamoto and T. Fukuda, *Solid State Sci.*, 2004, **6**, 879.